density than do equilibrium dimensions. The finding reported in this paper that lattice type does not materially affect the dynamical behavior, but that bead movement rules do, is perhaps not surprising in this regard. Further, these results raise the possibility that universal chain-length dependences of dynamical properties analogous to those found for equilibrium dimensions may simply not exist; i.e., nontrivial dependence upon move rules may be unavoidable.

Lastly, the chain-length dependences of D, τ_1, and $\langle l^2 \rangle$ track in such a way that the dimensionless ratio $D\tau_1 / \langle l^2 \rangle$ stays more or less constant, with about the same value calculated for a Rouse bead-spring model, independent of lattice, move rules, chain length, or excluded volume constraints. This ratio may be the sole universal quantity for dynamical properties.

References and Notes

(1) Verdier, P. H.; Stockmayer, W. H. *J. Chem. Phys.* **1962**, *36*, 227.
(2) Verdier, P. H. *J. Chem. Phys.* **1966**, *45*, 2122.
(3) Kranbuehl, D. E.; Verdier, P. H. *J. Chem. Phys.* **1972**, *56*, 3145.
(4) Verdier, P. H. *J. Chem. Phys.* **1973**, *59*, 6119.
(5) Kranbuehl, D. E.; Verdier, P. H. *J. Chem. Phys.* **1977**, *67*, 361.
(6) Hilhorst, H. J.; Deutch, J. M. *J. Chem. Phys.* **1975**, *63*, 5153.
(7) Boots, H.; Deutch, J. M. *J. Chem. Phys.* **1977**, *67*, 4608.
(8) Kranbuehl, D. E.; Verdier, P. H. *J. Chem. Phys.* **1979**, *71*, 2662.
(9) Kranbuehl, D. E.; Verdier, P. H. *Polym. Prepr.—Am. Chem. Soc.*, **1980**, *21*, 195.
(10) Gurler, M. T.; Crabb, C. C.; Dahlin, D. M.; Kovac, J. *Macromolecules* **1983**, *16*, 398.
(11) Stokely, C.; Crabb, C. C.; Kovac, J. *Macromolecules* **1986**, *19*, 860.
(12) Verdier, P. H. *J. Comput. Phys.* **1969**, *4*, 204.
(13) Throughout this paper, the word "random" with reference to computer simulations means the result of using a pseudorandom number generator. The generator employed in the present work was of the multiplicative congruential type, with a multiplier of 5^{13} and a modulus of 2^{35}.
(14) For $p = 0.5$ and $N = 99$, we obtain the value 0.0413 in units of N^3 move cycles. The correct value of $^0\tau_1$ for $p = 0.0$ and $N = 63$ is 0.1013, not 0.1010 as given in ref 8. (The corresponding ratio R in Table III of ref 8 should be 47.5 instead of 47.7.) The remaining values of $^0\tau_1$ are as reported in ref 8.
(15) Perico, A.; Bisio, S.; Cuniberti, C. *Macromolecules* **1984**, *17*, 2686.
(16) Rouse, P. E., Jr. *J. Chem. Phys.* **1953**, *21*, 1972. Zimm, B. H. *J. Chem. Phys.* **1956**, *24*, 269.
(17) Kranbuehl, D. E.; Verdier, P. H. *Macromolecules* **1984**, *17*, 749.
(18) Romiszowski, P.; Stockmayer, W. H. *J. Chem. Phys.* **1984**, *80*, 485.

Investigation of Local Motions in Polymers by the Dynamic Rotational Isomeric State Model

Ivet Bahar and Burak Erman*

*School of Engineering, Boğaziçi University, Bebek, 80815, Istanbul, Turkey.
Received July 15, 1986*

ABSTRACT: The internal dynamics of a short sequence in a chain is studied according to the dynamic isomeric state scheme. Conformational transitions with dynamic pair correlations are considered. Resistance to dynamic rearrangements resulting from environmental effects and constraints operating at the ends of a sequence is incorporated into the calculation scheme. Calculations for a short sequence in a polyethylene chain showed that pair correlations do not significantly affect the orientational relaxation of a vector affixed to a bond of the sequence. Contribution from constraints, on the other hand, is dominant and slows down the orientational motions.

Introduction

The Rouse–Zimm model,[1,2] though successful in representing the low-frequency motions of polymeric chains, is unsuitable for rapid relaxation processes that are attributed to local conformational transitions of the backbone. These motions are studied by techniques such as NMR, dielectric relaxation, fluorescence anisotropy decay, ESR, ultrasonic relaxation, dynamic light scattering, giving information about the orientation correlation functions and/or the corresponding spectral densities. A common feature deduced from experimental evidence is the occurrence of a nonexponential relaxation associated with local backbone rearrangements. To explain the observed departure from Debye behavior, on a molecular basis, stochastic jump models, both numerical[3-7] and analytical,[8-12] have been developed. In dynamic Monte Carlo techniques, Verdier and Stockmayer[3,4] and Gény and Monnerie[5] adhered to the postulate of local coordinated motion leaving unchanged the tails surrounding the mobile segment. Such crankshaft motions were first conceived by Boyer and Schatzki.[13] On the other hand, Helfand et al.[6-9] concentrated on the transitions of a single bond,

accompanied by some distortion and deformation spread over the neighboring units, in order to accommodate the newly created isomeric state. In fact, the experimentally observed[14-16] activation energies and Brownian simulations[6,7] suggest the crossing of but a single rotational barrier during local motions. According to their kinetic theory, which employs an extension of Kramer's rate theory,[17] compensating pair transitions are between second neighbors and occur only when the intervening bond is in the trans position. The two-state model proposed by Hall and Helfand[7] treats two types of transitions, cooperative and individual, leading respectively to compensating motions of neighboring units and translation of chain ends.

The basic physical and mathematical character of local chain dynamics is delineated in the above studies and in several references cited therein. The local dynamics may conveniently be described by the orientational relaxation of a vector affixed to a bond of the chain. That this relaxation progresses through correlated rotational transitions of the bonds of the sequence is now well established. However two fundamental points brought out by these studies still remain unsettled. First, the effect of neighbor

correlations on time correlation functions has to be assessed quantitatively. Mathematical treatments of neighbor correlations based on the dynamic Ising model[10,18-21] are essentially one-dimensional models and cannot be used to rationally describe the consequences of three-dimensional rotations about bonds. Second, the importance of constraints associated with chain connectivity and resistance of the surroundings has to be established on more quantitative grounds. On-lattice treatments that leave the tails of a sequence unchanged and local rearrangement models that do not impose constraints on the motion of the tails are two extremes.

The express purpose of the present study is to develop a mathematical scheme for calculating the effects of neighbor correlations and of constraints due to chain connectivity in a short sequence situated in a long polymeric chain. The mathematical model of Jernigan,[22] which is essentially the application of the rotational isomeric state scheme to chain dynamics, is adopted for this purpose. Accordingly, the internal time correlation functions of a chain can be computed by employing matrix methods previously used in calculations of equilibrium chain statistics.[23] The method is essentially an extension of the dynamic Ising model of Glauber[18] to real polymeric systems.

In the first section below, the problem is defined and the method of Jernigan is recapitulated with specific emphasis on dynamic pair correlations in a chain. In the following section, results of the theory are applied to investigate the internal dynamics of a long polyethylene chain. The autocorrelation of a vector affixed to the middle of a nine-bond sequence in the polyethylene chain is calculated. It should be pointed out that the "motional unit" in a relaxing chain is not defined a priori. Different length scales are probed in various spectroscopic experiments.[24] For instance, the motions of relatively short sequences are probed in NMR, whereas dielectric relaxation probes larger scale motions. The length scale of motional units is estimated to be approximately 7 times larger in dielectric relaxation compared to that in NMR.[25] Also recent holographic grating experiments[26] lead to correlation times ca. 8 times larger than those observed in NMR experiments. The complete description of local dynamics should include the contribution from motional units of various sizes. The choice of nine bonds in the present study is only for the purpose of illustration of the factors affecting the relaxation mechanism. The present exploratory analysis may be extended to longer sequences at the expense of computer time only.

Theory

Description of the Model. A short sequence AB in a long polymeric chain is depicted in Figure 1. The two portions PA and BQ of the chain on both sides of the sequence are shown with heavy dashed lines. A unit vector **m** is affixed to the middle bond of the sequence. The coordinate system Axyz is embedded in the chain. The x axis is chosen to lie along the first bond of the sequence. Th y axis is chosen such that second bond of the sequence lies in the xy plane. The vector **r** represents the instantaneous end-to-end vector of the sequence. A laboratory fixed-coordinate system is represented by OXYZ. The instantaneous position of point A with respect to the laboratory fixed-coordinate system is denoted by **R**.

The chain may be situated in a suitable solvent or may be in the bulk state above its glass–rubber transition temperature. In any event, the dynamics of the chain is assumed to result from rotational transitions of bonds from one isomeric state to the other. These isomeric transitions
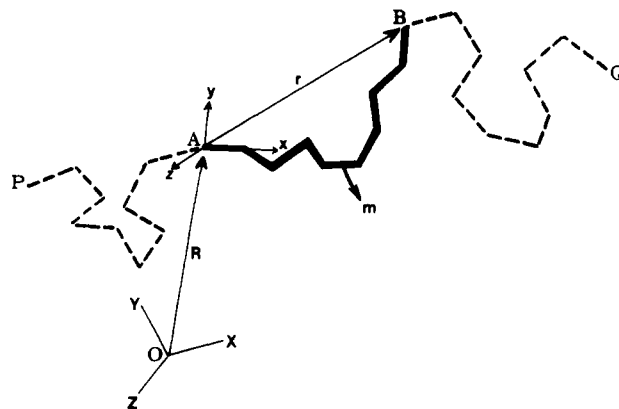

Figure 1. Schematic representation of a portion of the polymeric chain. A unit vector **m** is affixed to the central bond of the nine-bond sequence AB whose end-to-end vector is denoted **r**. The mobile frame Axyz is embedded in the chain as shown in the figure. OXYZ is the laboratory fixed-coordinate system. The vector **R** joins the centers of the two reference frames.

usually take place in the nanosecond range and involve coordinated motions of a few bonds only. The sequence AB shown in Figure 1 is chosen such that in the short duration of interest conformational rearrangements in the portions PA and BQ of the chain do not appreciably change the orientation of the vector **m**.

Let the orientational relaxation of **m** be described by a time correlation function $\Phi(t)$. Any such function observed in a spectroscopy experiment is necessarily expressed with respect to the laboratory fixed-coordinate system OXYZ. Two factors contribute to the orientational relaxation of **m**: (1) the internal relaxation due to the rotameric transitions in the bonds of the sequence AB, formulated with respect to a chain-embedded coordinate system such as Axyz; (2) the orientational relaxation of the coordinate system Axyz with respect to the laboratory fixed system OXYZ referred to as the external relaxation in the following.

With the assumption that the two contributions are uncorrelated, the function $\Phi(t)$ may be expressed as the product $\Phi(t) = \Phi_{ext}(t)\Phi_{int}(t)$, where $\Phi_{ext}(t)$ and $\Phi_{int}(t)$ are the external and internal correlation functions, respectively. The specific aim of the present study is the mathematical description of the internal relaxation function $\Phi_{int}(t)$ with respect to the chain-embedded coordinate system Axyz.

The internal time correlation function $\Phi_{int}(t)$ may stand for the internal parts of two experimentally measurable functions, defined as

$$M_{1,int}(t) = \langle \mathbf{m}(0) \cdot \mathbf{m}(t) \rangle \qquad (1)$$

and

$$M_{2,int}(t) = (1/2)\{3\langle [\mathbf{m}(0) \cdot \mathbf{m}(t)]^2 \rangle - 1\} \qquad (2)$$

where the argument of **m** denotes the time of observation and the dot denotes the scalar product. $M_{1,int}(t)$ is the internal autocorrelation function involved in dielectric relaxation, whereas $M_{2,int}(t)$ is the one involved in NMR, ESR, and fluorescence anisotropy experiments.

Recapitulation of Jernigan's Scheme. According to the rotational isomeric state theory,[23] each bond along the backbone is assumed to undergo a discrete angular rotation about its own axis. In general three rotations leading to configurations referred to as trans (t) and gauche $\pm$ (g$^{\pm}$) are found to be energetically most favorable. For a sequence consisting of N skeletal bonds, a complete set of rotational angles (ϕ_1, ϕ_2, ..., ϕ_N) specifies a given configuration, $\{\bar{\phi}\}_k$, $k = 1, 2, ..., 3^N$. We let $\mathbf{P}^{(N)}(t)$ denote the

3^N-dimensional vector of the time-dependent probabilities of all possible configurations $\{\tilde{\phi}\}_k$. The time rate of change of $\mathbf{P}^{(N)}(t)$ may be related to $\mathbf{P}^{(N)}(t)$ by a matrix equation known as the master equation

$$d\mathbf{P}^{(N)}(t)/dt = \mathbf{A}^{(N)}\mathbf{P}^{(N)}(t) \tag{3}$$

where $\mathbf{A}^{(N)}$ is the $3^N \times 3^N$ matrix with the element $A_{kl}^{(N)}$ describing the momentary rate of passage from configuration $\{\tilde{\phi}\}_l$ to $\{\tilde{\phi}\}_k$. Equation 3 may be solved formally to yield

$$\mathbf{P}^{(N)}(t) = \exp(\mathbf{A}^{(N)}t)\mathbf{P}^{(N)}(t{=}0) =$$
$$\mathcal{B}^{(N)} \exp(\mathcal{L}^{(N)}t)[\mathcal{B}^{(N)}]^{-1}\mathbf{P}^{(N)}(t{=}0) = \mathcal{C}^{(N)}\mathbf{P}^{(N)}(t{=}0) \tag{4}$$

where $\mathcal{B}^{(N)}$ is the matrix formed from eigenvectors of $\mathbf{A}^{(N)}$, $\mathcal{L}^{(N)}$ is the diagonal matrix of eigenvalues of $\mathbf{A}^{(N)}$, $[\mathcal{B}^{(N)}]^{-1}$ is the inverse of $\mathcal{B}^{(N)}$ and

$$\mathcal{C}^{(N)} \equiv \mathcal{B}^{(N)} \exp(\mathcal{L}^{(N)}t)[\mathcal{B}^{(N)}]^{-1} \tag{5}$$

is the time-dependent (or delayed) conditional probability matrix.

The element $\mathcal{C}_{kl}^{(N)}$ denotes the conditional probability of the occurrence of configuration $\{\tilde{\phi}\}_k$ at time t, assuming that the configuration was $\{\tilde{\phi}\}_l$ at $t = 0$. It is evident from this definition that the elements of each column sum up to unity since they encompass all possible transitions starting from a fixed initial configuration.[27] The total time-dependent joint probability matrix $\mathcal{P}^{(N)}$ is given in terms of $\mathcal{C}^{(N)}$ as

$$\mathcal{P}^{(N)} = \mathcal{C}^{(N)} \operatorname{diag} \mathbf{P}^{(N)}(t{=}0) \tag{6}$$

The element $\mathcal{P}_{kl}^{(N)}$ denotes the joint probability of having configuration $\{\tilde{\phi}\}_k$ at time t and $\{\tilde{\phi}\}_l$ at $t = 0$. Knowledge of $\mathcal{P}^{(N)}$ leads to a complete description of the dynamics of the N-bond sequence.
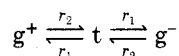
Consider the rotation of a single bond. The rotating bond is allowed to assume any conformational state (t, g$^+$, g$^-$) irrespective of the state of the adjacent bonds. For single bond motion, the master equation reduces to

$$d\mathbf{P}_j^{(1)}(t)/dt = \mathbf{A}_j^{(1)}\mathbf{P}_j^{(1)}(t) \tag{7}$$

The subscripts index the location of the mobile bond along the long polymeric chain. The associated relationships given by eq 4–6 equally apply with the superscript (1) replacing (N). $\mathcal{B}^{(1)}$, $\mathcal{L}^{(1)}$, and $\mathcal{P}^{(1)}$ retain their previous definitions. In particular, the elements of $\mathcal{P}^{(1)}$ will be denoted by $p(\zeta,t;\zeta',0)$ and represent the joint probability of occurrence of state ζ at time t and ζ' at $t = 0$.

If the mobile bond undergoes independent conformational transitions according to Scheme I[22]

Scheme I

$$g^+ \underset{r_1}{\overset{r_2}{\rightleftharpoons}} t \underset{r_2}{\overset{r_1}{\rightleftharpoons}} g^-$$

as in polyethylene, the matrix $\mathbf{A}^{(1)}$ takes the form[22]

$$\mathbf{A}^{(1)} = \begin{bmatrix} -2r_1 & r_2 & r_2 \\ r_1 & -r_2 & 0 \\ r_1 & 0 & -r_2 \end{bmatrix} \tag{8}$$

Here r_1 and r_2 denote the rates of the transitions indicated in Scheme I. For N-bond sequences obeying independent stochastics, the vector $\mathbf{P}^{(N)}(t)$ may be written[22]

$$\mathbf{P}^{(N)}(t) =$$
$$\mathbf{P}_1^{(1)}(t) \otimes \mathbf{P}_2^{(1)}(t) \otimes \dots \otimes \mathbf{P}_j^{(1)} \otimes \dots \otimes \mathbf{P}_{N-1}^{(1)}(t) \otimes \mathbf{P}_N^{(1)}(t) \tag{9}$$

where $\otimes$ denotes the direct product. Differentiating both sides of eq 9 with respect to time and using eq 7, we end up with the master equation for the N-bond sequence with independent bond rotations

$$d\mathbf{P}^{(N)}(t)/dt =$$
$$\sum_{j=1}^{N} (\mathbf{I}_3 \otimes \mathbf{I}_3 \otimes \dots \otimes \mathbf{A}_j^{(1)} \otimes \dots \otimes \mathbf{I}_3 \otimes \mathbf{I}_3)\mathbf{P}^{(N)}(t) \tag{10}$$

where $\mathbf{I}_3$ is the third-order identity matrix. The corresponding joint probability matrix $\mathcal{P}^{(N)}$ was determined by Jernigan, using the procedure outlined by eq 4–6. The neighbor dependence of equilibrium statistics was incorporated into the treatment through adoption of interdependent equilibrium distribution for $\mathbf{P}^{(N)}(t{=}0)$.

Pairwise-Dependent Transitions. If simultaneous transitions of the jth and $(j + 1)$th bond are considered, the master equation takes the following form:

$$d\mathbf{P}^{(N)}(t)/dt =$$
$$\{\sum_{j=1}^{N} \mathbf{I}_3 \otimes \mathbf{I}_3 \otimes \dots \otimes \mathbf{A}_{j,j+1}^{(2)} \otimes \dots \otimes \mathbf{I}_3 \otimes \mathbf{I}_3\}\mathbf{P}^{(N)}(t) \tag{11}$$

Equation 11 holds for sequences of bonds with independent statistics but pairwise-dependent dynamics. The elements of $\mathbf{A}_{j,j+1}^{(2)}$ are the transition rates from one pair of isomeric states to the other. $\mathbf{A}_{j,j+1}^{(2)}$ is related to the bond probabilities by the expression

$$d[\mathbf{P}_j^{(1)}(t) \otimes \mathbf{P}_{j+1}^{(1)}(t)]/dt = \mathbf{A}_{j,j+1}^{(2)}\mathbf{P}_j^{(1)}(t) \otimes \mathbf{P}_{j+1}^{(1)}(t) \tag{12}$$

However not all of the transitions are accessible owing to high energy barriers between conformers. Consequently, a number of elements in the matrix $\mathbf{A}_{j,j+1}^{(2)}$ equate to zero. Conformational energy maps constructed by varying two successive skeletal bonds may be used to localize the bounded region of permitted pair transitions; this region is in general surrounded by high-energy walls. Within the domain of accessible transitions, passage from one configuration to another occurs through saddle points. For example, the examination of energy maps[28] for polyethylene suggests the accessible transitions shown in Scheme II. r_1, r_2, and r_3 denote the indicated rates of transitions. r_{-i} refers to the rate in the opposite sense of r_i. Explicit expressions for the rates will be given in the next section. Following Scheme II, $\mathbf{A}_{j,j+1}^{(2)}$ becomes the matrix shown in eq 13.

Inasmuch as the sequence is assumed to be inside a long chain, the subscripts $j,j+1$ will be omitted in the following. The matrix $\mathbf{A}^{(2)}$ may be used to calculate the matrices $\mathcal{B}^{(2)}$, $\mathcal{L}^{(2)}$, $\mathcal{C}^{(2)}$, and $\mathcal{P}^{(2)}$ in analogy with the procedure outlined above for $N = 1$. The elements $p(\zeta\eta,t;\zeta'\eta',0)$ of $\mathcal{P}^{(2)}$ give the joint probability of state $\zeta\eta$ at time t and $\zeta'\eta'$ at $t = 0$ for a given pair of bonds.

$$\mathbf{A}_{j,j+1}^{(2)} = \begin{bmatrix} -4r_1 & r_{-1} & r_{-1} & r_{-1} & 0 & 0 & r_{-1} & 0 & 0 \\ r_1 & -r_2-r_3-r_{-1} & 0 & 0 & r_{-2} & 0 & 0 & r_{-3} & 0 \\ r_1 & 0 & -r_2-r_3-r_{-1} & 0 & 0 & r_{-3} & 0 & 0 & r_{-2} \\ r_1 & 0 & 0 & -r_2-r_3-r_{-1} & r_{-2} & r_{-3} & 0 & 0 & 0 \\ 0 & r_2 & 0 & r_2 & -2r_{-2} & 0 & 0 & 0 & 0 \\ 0 & 0 & r_3 & r_3 & 0 & -2r_{-3} & 0 & 0 & 0 \\ r_1 & 0 & 0 & 0 & 0 & 0 & -r_2-r_3-r_{-1} & r_{-3} & r_{-2} \\ 0 & r_3 & 0 & 0 & 0 & 0 & r_3 & -2r_{-3} & 0 \\ 0 & 0 & r_2 & 0 & 0 & 0 & r_2 & 0 & -2r_{-2} \end{bmatrix} \tag{13}$$

Scheme II

Calculation of the Rates r_i. The explicit expressions for the rates r_i consist of the product of two terms: one reflecting the height E_a of the saddle point to be crossed with respect to the initial isomeric state and the other accounting for the frictional drag exerted by the medium. The first one is the familiar Boltzmann factor while the second one enters as a front factor. This front factor requires some elucidation. Jernigan chose the front factor to be of the form $k_B T/h$, where k_B is the Boltzman constant, h, Planck's constant, and T the absolute temperature, in conformity with Eyring's theory of absolute reaction rates.[29] This factor represents the frequency with which the activated complex crosses the energy barrier at a given temperature. According to the theory,[29] this factor is multiplied by the ratio (F^*/F) of the partition function of the molecule in the activated state to that in the initial state. Written in explicit form, the correct expression for the rate will be

$$r = (k_B T/h)(F^*/F) \exp\{-E_a/RT\} \quad (14)$$

and the ratio F^*/F is given by[29]

$$F^*/F = (h^2/2\pi m k_B T)^{1/2}/v_f^{1/3} \quad (15)$$

where m is the mass of the particle undergoing the transition and moving in the free volume v_f. The free volume v_f of a particle oscillating in a potential well is proportional to the amplitude of the harmonic motion. This amplitude d may be expressed in terms of the force constant γ, which is a measure of the relative steepness of the potential well, as

$$d = (2\pi k_B T/\gamma)^{1/2} \quad (16)$$

so that

$$v_f^{1/3} \propto (2\pi k_B T/\gamma)^{1/2} \quad (17)$$

where $\propto$ denotes the proportionality.

In the theory of absolute reaction rates the crossing over the potential barrier is the rate-controlling event. In analogy with eq 16, we may write for the top of the barrier[8,9]

$$d^* = (2\pi k_B T/\gamma^*)^{1/2} \quad (18)$$

where d^* and γ^* are characteristics of the activated state.

Substituting eq 15 and 17 in eq 14, we obtain Kramers'[17] low friction rate expression

$$r = (1/2\pi)(\gamma/m)^{1/2} \exp\{-E_a/RT\} \quad (19)$$

In this low friction limit, which does not include the friction coefficient ζ, the particle flows over the barrier with an average velocity equal to $(k_B T/2\pi m)^{1/2}$, assuming that there is equilibrium distribution of velocities in the activated state. If J denotes the flux over the barrier and n^* the density of the particles across the barrier, the velocity in the low-friction limit may be written as

$$J/n^* = (k_B T/2\pi m)^{1/2} \quad (20)$$

In the other extreme case of high-friction limit the same quantity becomes[8,9]

$$J/n^* = D/d^* \quad (21)$$

where the diffusion constant is given by

$$D = k_B T/\zeta \quad (22)$$

Using eq 18-22, we end up with Kramers' expression for the rate in the high-friction medium

$$r = (\gamma\gamma^*)^{1/2}(2\pi\zeta)^{-1} \exp\{-E_a/RT\} \quad (23)$$

The same equation was adopted by Helfand and Skolnick[9] in their kinetic treatment of conformational transitions in polymers. A general expression for the rate of transition applicable at low, intermediate, and high friction can be found in their work.[9]

Through adoption of eq 23, the rotational transition rates are rendered ca. 20 times slower compared to those resulting from Jernigan's treatment where the ratio F^*/F in eq 14 is not considered, thus leading to too rapid motions.

Solution of the Master Equation for a Sequence with Pairwise Cooperative Transitions. The elements of the joint probability matrix $\mathcal{P}^{(N)}(t)$ may be written explicitly for the case of pairwise-dependent bonds. Consider, for instance, the following transition:

$$(\alpha'\beta'\gamma'\delta'...;0) \rightarrow (\alpha\beta\gamma\delta...;t)$$

where $\alpha'\beta'\gamma'\delta'...$ denotes the state of the sequence at $t = 0$ and $\alpha\beta\gamma\delta...$ denotes that at time t. The corresponding joint probability or equivalently the normalized stochastic weight associated with this transition will be

$$p(\alpha\beta\gamma\delta...t;\alpha'\beta'\gamma'\delta...0) = \\ p(\alpha\beta,t;\alpha'\beta',0)q(\beta\gamma,t;\beta'\gamma',0)q(\gamma\delta,t;\gamma'\delta',0)... \quad (24)$$

where

$$q(\beta\gamma,t;\beta'\gamma',0) = p(\beta\gamma,t;\beta'\gamma',0)/[\sum_\eta \sum_\zeta p(\beta\eta,t;\beta'\zeta',0)] \quad (25)$$

The summation in eq 25 is over all possible rotational states. Thus, if three isomeric states are available to each bond, this summation includes nine terms ($\eta = $ t,g$^+$,g$^-$ and $\zeta' = $ t,g$^+$,g$^-$). The term $q(\beta\gamma,t;\beta'\gamma',0)$ may be viewed as the conditional probability of occurrence of the joint event $(\beta\gamma,t;\beta'\gamma',0)$, given that the first bond of the pair undergoes the transition from initial state β' to state β at time t. Thus $q > p$, since the sample space is reduced by fixing the initial and final states of the first bond of the pair. The application of eq 24 and 25 to every possible transitions ($3^N \times 3^N$ of them for N bonds with three states, each) yields the time-delayed joint probability matrix $\mathcal{P}^{(N)}(t)$.

For independent bonds undergoing independent transitions, eq 24 simplifies to

$$p(\alpha\beta\gamma\delta...t;\alpha'\beta'\gamma'\delta'...0) = \\ p(\alpha,t;\alpha',0)p(\beta,t;\beta',0)p(\gamma,t;\gamma',0)p(\delta,t;\delta',0)... \quad (26)$$

where $p(\alpha,t;\alpha,0)$, $p(\beta,t;\beta',0)$, etc., are elements of the matrix $\mathcal{P}^{(1)}(t)$.

Effect of Constraints. Let $\mathbf{r}(0)$ and $\mathbf{r}(t)$ denote the end-to-end vector of the sequence at $t = 0$ and t, respectively. The fluctuation in $\mathbf{r}$ during this time interval is

$$\Delta\mathbf{r} = \mathbf{r}(t) - \mathbf{r}(0) \quad (27)$$

Let the motion of the sequence be described with respect to the coordinate system Axyz shown in Figure 1. If there are no constaints operating on end B of the sequence shown in Figure 1, then $\Delta\mathbf{r}$ will take any value compatible with conformational transitions available to the sequence

AB. If, on the other hand, the motion of end B relative to end A is constrained by the presence of the sequence BQ of the chain, Δr will be confined to within a spherical domain defined by $\Delta r < \delta_0$, where Δr is the magnitude of Δr and δ_0 denotes the radius of the sphere in which the end B may travel between successive transitions. δ_0 varies inversely with the strength of constraints.

Confinement of Δr into a sphere excludes certain conformational transitions of the chain which would otherwise be possible in the absence of constraints. If, for example, the transition from configuration $\{\tilde{\phi}\}_l$ at time $t = 0$ to $\{\tilde{\phi}\}_k$ at time t renders $\Delta r > \delta_0$, the element $\mathcal{P}_{kl}^{(N)}$ of $\mathcal{P}^{(N)}(t)$ has to be replaced by zero. The elements of $\mathcal{P}^{(N)}$ obtained in this manner have to be renormalized to yield $\sum_k \sum_l \mathcal{P}_{kl}^{(N)} = 1$.

Expressions for Orientational Autocorrelation Functions. The time-dependent joint probability matrix $\mathcal{P}^{(N)}(t)$ may be used to calculate the autocorrelation function $M_{1,\text{int}}(t)$ of **m** as

$$M_{1,\text{int}}(t) = \mathcal{M}^{\mathrm{T}}(\mathcal{P}^{(N)}(t) \otimes \mathbf{I}_3)\mathcal{M} \qquad (28)$$

Here, the superscript T denotes the transpose, and

$$\mathcal{M} \equiv \begin{bmatrix} \mathbf{m}_1 \\ \mathbf{m}_2 \\ \cdot \\ \cdot \\ \cdot \\ \mathbf{m}_j \\ \cdot \\ \cdot \\ \cdot \\ \mathbf{m}_{3^N} \end{bmatrix} \qquad (29)$$

where $\mathbf{m}_j$ is the vector **m** corresponding to configuration $\{\tilde{\phi}\}_j$.

Equation 28 may be expressed in component form as

$$M_{1,\text{int}}(t) = \sum_i \sum_j \mathcal{P}_{ij}^{(N)} \, \mathbf{m}_i \cdot \mathbf{m}_j \qquad (28')$$

where the summations are over all available configurational states of the chain.

The second orientational autocorrelation function $M_{2,\text{int}}(t)$ may be expressed in matrix form as

$$M_{2,\text{int}}(t) = \tfrac{1}{2}\{3 \, \mathrm{Tr} \, (\mathcal{N}^{\mathrm{T}}(\mathcal{P}^{(N)}(t) \otimes \mathbf{I}_3)\mathcal{N}) - 1\} \quad (30)$$

where Tr denotes the trace operator and $\mathcal{N}$ is the $3^{N+1} \times 3$ matrix defined by

$$\mathcal{N} \equiv \begin{bmatrix} \mathbf{m}_1 \mathbf{m}_1^{\mathrm{T}} \\ \mathbf{m}_2 \mathbf{m}_2^{\mathrm{T}} \\ \cdot \\ \cdot \\ \mathbf{m}_{3^N} \mathbf{m}_{3^N}^{\mathrm{T}} \end{bmatrix} \qquad (31)$$

Equation 30 may be written in component form as

$$M_{2,\text{int}}(t) = \tfrac{1}{2}\{3 \sum_i \sum_j \mathcal{P}_{ij}^{(N)} \, (\mathbf{m}_i \cdot \mathbf{m}_j)^2 - 1\} \qquad (30')$$

Calculations for the Polyethylene Chain

Various sequences of different sizes contribute to the internal relaxation of a chain, thus affecting the experimentally observed spectra. Calculations for the internal relaxation of a sequence of nine bonds of a polyethylene chain are presented in the following, for illustrative purposes.

Conformational energies determining rotational states are taken from the work of Abe, Jernigan, and Flory.[28] Only the internal dynamics relative to the reference frame Axyz is considered. The first bond of the sequence is held

Table I
Most Probable Transitions

no.	transition, $\zeta'\eta' \rightarrow \zeta\eta$
1	tt $\rightarrow$ tt
2	tg$^\pm$ $\rightarrow$ tg$^\pm$
	g$^\pm$t $\rightarrow$ g$^\pm$t
3	g$^\pm$g$^\pm$ $\rightarrow$ g$^\pm$g$^\pm$
4	g$^\pm$g$^\mp$ $\rightarrow$ g$^\pm$g$^\mp$
5	g$^\pm$t $\rightarrow$ tt
	tg$^\pm$ $\rightarrow$ tt
6	tt $\rightarrow$ tg$^\pm$
	tt $\rightarrow$ g$^\pm$t
7	g$^\pm$g$^\pm$ $\rightarrow$ tg$^\pm$
	g$^\pm$g$^\pm$ $\rightarrow$ g$^\pm$t
8	g$^\pm$g$^\mp$ $\rightarrow$ g$^\pm$t
	g$^\pm$g$^\mp$ $\rightarrow$ tg$^\pm$
9	g$^\pm$g$^\mp$ $\rightarrow$ tt
10	g$^\mp$t $\rightarrow$ tg$^\pm$
	tg$^\pm$ $\rightarrow$ g$^\mp$t

fixed in the trans state. The dynamics of **m** is expressed in terms of the second internal autocorrelation function $M_{2,\text{int}}(t)$. In the absence of constraints at the end B, the dynamics of **m** is determined by the transitions of the bonds situated between point A and **m**. The remaining part of the sequence between **m** and point B is inconsequential for the unconstrained motions. The whole sequence, however, has to be considered in the presence of constraints due to the non-Markoffian nature of the phenomenon.

Calculation of Conditional Pair Probabilities. The time-dependent conditional probability matrix for pairs of polyethylene bonds is calculated form eq 5, with $N = 2$. $\mathcal{B}^{(2)}$ and $\mathcal{L}^{(2)}$ in eq 5 are computed by similarity transformation from $\mathbf{A}^{(2)}$ defined by eq 13. The rates in $\mathbf{A}^{(2)}$ were obtained with eq 23. The values for γ, γ^*, and ζ for polyethylene were taken from ref 9. The front factor $(\gamma\gamma^*)^{1/2}/2\pi\zeta$ was calculated to be 2.77×10^{11} s^{-1}. The activation energies for the rates r_1, r_{-1}, r_2, r_{-2}, r_3, and r_{-3} were taken as 3.5, 3.0, 3.7, 3.0, 3.0, and 0.3 kcal/mol, respectively, as deduced from the heights of the saddle points of energy maps constructed[28] for polyethylene. Detailed calculations of the energy map show that the g$^\pm$g$^-$ states further split into two minima.[28] This splitting is however neglected within the approximation of equilibrium rotational isomeric states calculations. It is also assumed that this splitting does not significantly affect the local dynamics and is henceforth neglected.

Figure 2 displays the variation with time of the conditional probabilities for the pairs of bonds at 300 K. The elements of $\mathcal{C}^{(2)}$ are represented by $p(\zeta\eta,t/\zeta'\eta',0)$ in the ordinate. $p(\zeta\eta,t/\zeta'\eta',0)$ denotes the conditional probability of occurrence of states $\zeta\eta$ at time t given state $\zeta'\eta'$ at $t = 0$ for any pair of adjacent bonds. Only the most probable transitions are shown in the figures for the interest of clarity. The transitions are identified by numbers defined in Table I.

For comparison, the same conditional probabilities calculated on the basis of independent rotations are plotted in Figure 3. The matrix $\mathbf{A}^{(2)}$ for independent bonds was calculated from

$$\mathbf{A}^{(2)} = \mathbf{A}^{(1)} \otimes \mathbf{I}_3 + \mathbf{I}_3 \otimes \mathbf{A}^{(1)} \qquad (32)$$

as follows from eq 10. $\mathbf{A}^{(1)}$ is given by eq 8 where the rates were evaluated with eq 26 again with the same front factor as above and taking the activation energies for r_1 and r_2 equal to 3.5 and 3.0 kcal/mol, respectively. The associated matrix $\mathcal{C}^{(2)}$ for independent rotations is determined from $\mathbf{A}^{(2)}$ in eq 32, by the procedure outlined above.

Examination of Figures 2 and 3 leads to the following conclusions. The strong tendency of interdependent bonds
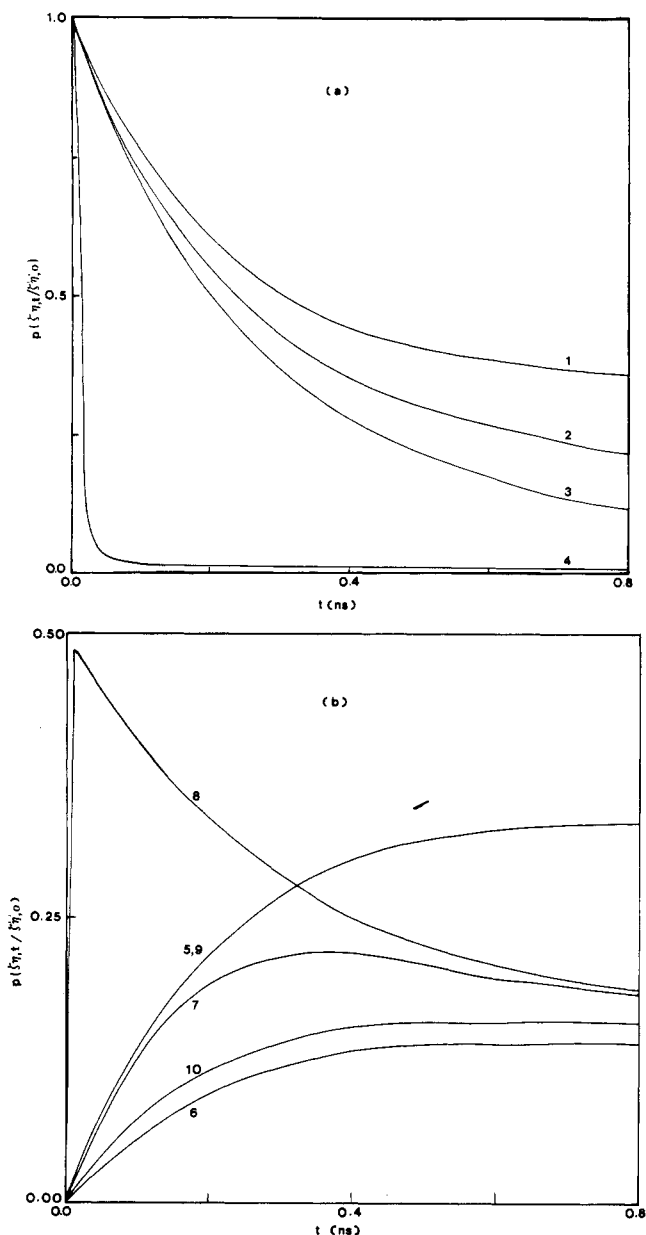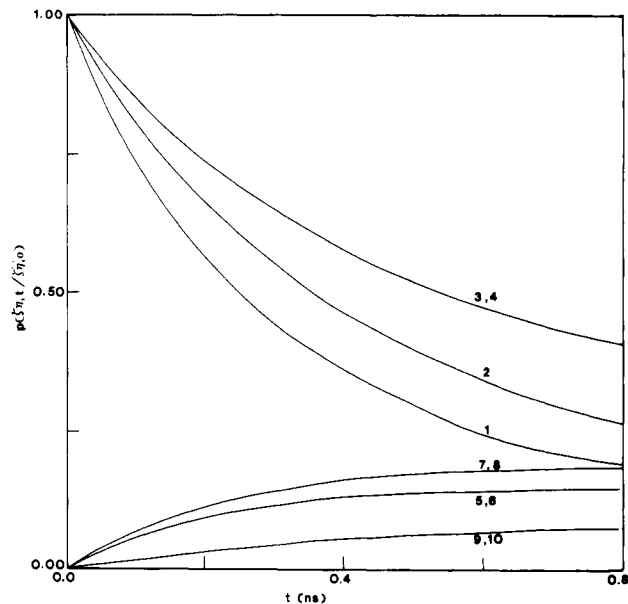
Figure 2. Time-dependent conditional probabilities $p(\zeta\eta,t;\zeta'\eta',0)$ for polyethylene bond pairs with interdependent rotational potentials. The curves are drawn for cases (a) $\zeta\eta = \zeta'\eta'$ and (b) $\zeta\eta \neq \zeta'\eta'$. The numbers on each curve indicate the transitions listed in Table I.

Figure 3. Time-dependent conditional probabilities $p(\zeta\eta,t;\zeta'\eta',0)$ for polyethylene bond pairs with independent rotational potentials. The numbers on each curve indicate the transitions listed in Table I.

to escape the $g^{\mp}g^{\pm}$ state constitutes the most apparent departure from the behavior of independent pairs. Resulting from this tendency, some transitions such as $g^{\pm}$ t $\rightarrow$ tg$^{\mp}$ and $g^{\pm}g^{\mp}$ $\rightarrow$ tt become relatively more important when neighbor dependence is taken into account. In general, the rates of transitions from state $\zeta\eta$ to $\zeta'\eta'$ are slightly enhanced with the introduction of neighboring bond interdependence. This increase in rate is however counterbalanced by the increased probability of pairs in tt state (the most probable state from equilibrium statistics) to remain unchanged. Thus although the character of the conditional probabilities depicted in Figures 2 and 3 differ markedly, this difference may not be reflected so significantly on the overall dynamic behavior in particular on the orientational autocorrelation function as will be shown below.

Calculations were carried out for 300 K in Figures 2 and 3. At this temperature, the probabilities converge to their equilibrium value within time intervals of about 1 ns, as

may be predicted from the extrapolation of the curves in Figures 2 and 3. Subsequent calculations will show that the relaxation time increases significantly with decreasing temperature.

Calculation of $M_{2,\text{int}}(t)$ for a Sequence without Constraints. The motion of **m** with respect to the coordinate frame Axyz is considered. The orientation of **m** relative to this frame is determined by the rotations of the five intervening bonds. Since the first bond is held in trans position, 3^4 configurations resulting from the isomeric rotations of the subsequent four bonds need be considered. If, as in the present study, the direction of **m** coincides with that of the central bond, the problem reduces to the analysis of the 3^3 configurations associated with the isomeric rotations of the three preceding bonds and the transitions in between. The vector $\mathbf{m}_i$ corresponding to configuration $\{\tilde{\phi}\}_i$ is determined by conventional methods employing bond-based coordinate frames and transformation matrices.[23] The transitions between all configurations are assigned time-dependent joint probability $\mathcal{P}_{ij}^{(N)}$ values according to eq 24 and 25. The joint probabilities for the pairs in eq 24 and 25 are determined from eq 6 with $N = 2$, where the conditional probability matrix $\mathcal{C}^{(2)}$ calculated in the above section for interdependent bonds is used. The components of $\mathbf{P}^{(2)}(t=0)$ in eq 6 follow from the equilibrium statistics of pairwise-dependent polyethylene chains.[23,28] The orientational autocorrelation function $M_{2,\text{int}}(t)$ is computed with eq 30' where the calculated $\mathcal{P}_{ij}^{(N)}$ and $\mathbf{m}_i$ values are substituted. Term-by-term evaluation of $\mathcal{P}^{(N)}$ (or $\mathcal{P}_{ij}^{(N)}$) in the manner stated above does not require the use of the complete matrix and hence allows for the extension to longer sequences, at the expense of computation time only.

The calculated orientational autocorrelation functions for interdependent rotations are represented by the solid curves in Figure 4 for $T = 200$, 250, and 300 K. A strong dependence on temperature is discernible. It is interesting to note that the autocorrelation functions do not relax to zero but to finite values representing the equilibrium autocorrelation of **m**.

To estimate the influence of neighbor dependence on the dynamics of the chain, the calculation of $M_{2,\text{int}}(t)$ was repeated for a sequence with independent bonds. In this
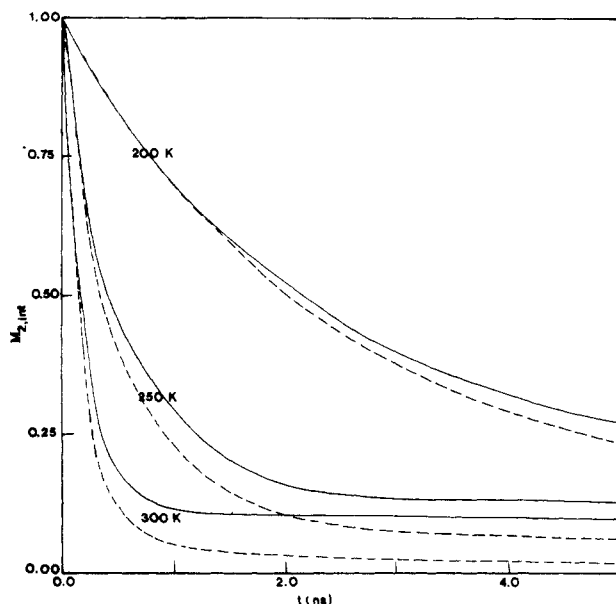
Figure 4. Orientational autocorrelation function $M_{2,int}(t)$ of the vector **m** in polyethylene at 200, 250, and 300 K. The solid curves are drawn for sequences with interdependent bonds. The dashed curves were calculated on the basis of independent rotational potentials. In calculations, end A of the sequence AB was held fixed, while the motion of B was not restricted.

case, $\mathcal{P}_{ij}{}^{(N)}$ values were determined from eq 26. The elements $p(\zeta,t;\zeta',0)$ of $\mathcal{P}^{(1)}$ in eq 26 were calculated from $\mathcal{P}^{(1)} = \mathcal{C}^{(1)}$ diag $\mathbf{P}^{(1)}(t=0)$, i.e., the form eq 6 takes for $N = 1$. The explicit expression for $\mathcal{C}^{(1)}$ is given in ref 22. The components of $\mathbf{P}^{(1)}(t=0)$ are taken as the equilibrium probabilities of t,g^+ and g^- states. Again eq 30 was used for the computation of $M_{2,int}(t)$ but, in this case, with the newly obtained $\mathcal{P}_{ij}$s. The resulting autocorrelation functions are shown as dashed curves in Figure 4.

The difference between the solid and the dashed curves increases as the equilibrium values are approached, while they follow almost the same trend during the initial stage of decay. Examination of the steps in the calculations shows that, although the same trend is observed during the decay of the autocorrelation functions, the contributions of specific transitions to $M_{2,int}(t)$ differ in the two treatments but finally sum to almost the same values for $M_{2,int}(t)$. The departures near equilibrium are however dominated by differing equilibrium distributions of independent and pairwise-dependent bonds.

Incorporation of pairwise dependence into equilibrium distributions as was done by Jernigan[22] is expected to lead to virtually the same solid curves as those depicted in Figure 4.

Calculation of $M_{2,int}(t)$ for a Sequence with Constraints. In this section, the autocorrelation function $M_{2,int}(t)$ is calculated for a nine-bond polyethylene sequence in which the fluctuations of end B (see Figure 1) of the sequence are restricted to values less than 3 Å.

The strength of constraints operating at point B of the sequence shown in Figure 1 is determined by the parameter δ_0, which restricts the possible configurational transitions. Accordingly, a transition that results in the displacement of end B larger than δ_0 has to be discarded from calculations. $\delta_0 = 0$ corresponds to one extreme case where the dynamics of the chain is realized only through reorganizations that leave the tails undisturbed. This situation corresponds to the on-lattice model of chain dynamics. The condition $\delta_0 = 0$ imposes severe constraints on the dynamics of a sequence. The smallest sequence for which this condition is satisfied contains three bonds as was
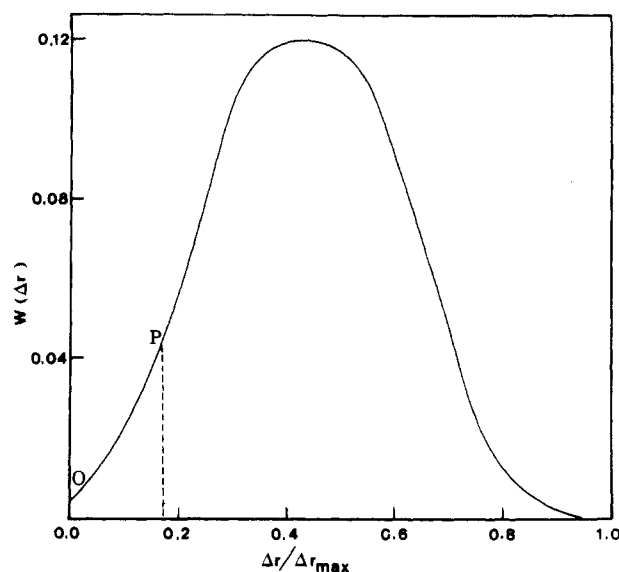

Figure 5. Distribution $W(\Delta r)$ of transitions in a sequence resulting in the displacement of one end by Δr, the other end being fixed. Calculations are performed for the nine-bond sequence. Point P denotes a displacement of 3 Å.

discussed by Monnerie et al.[5] some years ago. The number of allowable transitions satisfying the condition $\delta = 0$ is very small. Most of these transitions are crankshaft motions. The number of possible transitions increases significantly as end B of the sequence in Figure 1 is allowed to move in a finite domain. The other extreme case is the one in which end B may fluctuate freely. This corresponds to the case $\delta = \Delta r_{max}$, where Δr_{max} represents the maximum attainable distance between two positions of point B. In general, augmenting the size of the motional unit and decreasing the degree of constraints have qualitatively same effect on local dynamics.

The value of $\delta_0 = 3$ Å adopted in this section for the nine-bond polyethylene sequence is considerably smaller than the maximum value Δr_{max} of 17.54 Å. However, a significant number of transitions is possible with this choice of δ_0 as explained in the following paragraph.

Let $N(\Delta r)$ denote the number of transitions of a sequence which results in the displacement of end B by an amount Δr. The ratio of $N(\Delta r)$ to the total number of possible transitions describes the distribution, $W(\Delta r)$, of fluctuations resulting in a displacement of Δr. In Figure 5 results of calculations of this distribution for the nine-bond polyethylene sequence are shown as a function of Δr. The abscissa values are normalized by dividing Δr with Δr_{max}. The total possible number of transitions in the absence of constraints is 3^{14} for the nine-bond sequence in which the first bond is kept in the trans state and the state of the last bond does not affect the configurations of the sequence. Point P on the abscissa corresponds to the value of $\Delta r = 3$ Å. The total number of transitions with $\Delta r < \delta_0 = 3$ Å can be obtained from the area under the $W(\Delta r)$ curve between points 0 and P. Calculations show that 15% of the possible transitions are allowed under the constraint $\Delta r < 3$ Å.

The time dependence of the orientation autocorrelation function for a sequence with $\delta_0 = 3$ Å is shown in Figure 6 for three different temperatures.

Comparison of Figures 4 and 6 shows that relaxation is significantly slowed down when transitions are constrained, and the asymptotic values to which the curves converge are considerably higher in restricted motion. This result is a natural consequence of chain connectivity. The experimentally observed decay to zero is not obtainable
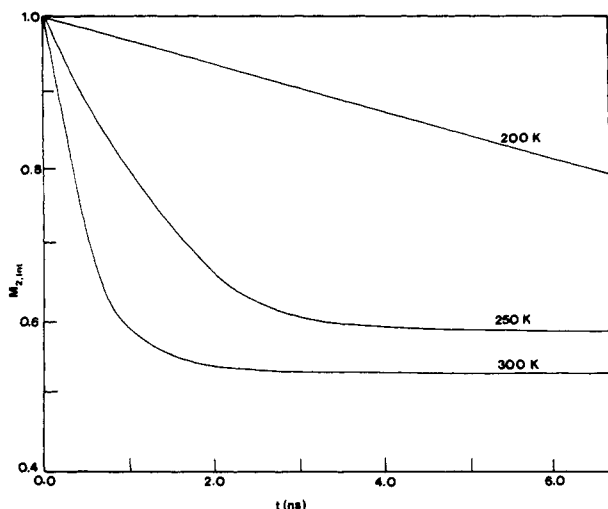
Figure 6. Orientational autocorrelation function $M_{2,int}(t)$ under restricted motion. End B is allowed to be displaced within a sphere of radius $\delta_0 = 3$ Å only. The curves are found to converge to substantially higher values compared to those in Figure 4 where no constraint due to chain connectivity operates on the motion of end B.

unless the overall external orientation of the chain is incorporated into the calculations. The loss of orientation caused by external rotation is operative when the time scale of observation matches that of overall reorientation. In fact, in fluorescence anisotropy decay experiments carried out with labeled alkyl chains, in the time scale of observation which probably does not allow for external relaxation, the autocorrelation function was observed to remain higher than zero, for C_{16}.[31]

Discussion and Conclusion

Conformational characteristics of real polymeric chains are incorporated into the treatment of the local dynamics associated with the internal orientational rearrangements of finite sequences within the chain. The treatment developed in the present study offers a convenient and realistic method for determining the elements of the time-delayed joint probability matrix $\mathcal{P}^{(N)}(t)$ which fully describes the conformational transitions of the investigated segment and may be used to calculate the time dependence of the internal orientational autocorrelation function $M_{2,int}(t)$.

The mathematical scheme developed in the present study is used to investigate the influence of factors such as neighbor correlations and constraints due to chain connectivity, on local dynamics.

To assess the effect of neighbor correlations, the autocorrelation functions for sequences with pairwise-dependent bonds were compared to those for sequences with independent bonds. Results of calculations at various temperatures are shown in Figure 4. The autocorrelation functions decay faster for sequences with independent bonds. The effect of pair dependence is not, however, as important as that arising from constraints operating at the ends of the motional unit (see below).

Inasmuch as transitions between isomeric states were assumed to occur through saddle points in 2-dimensional energy maps, the present calculation scheme does not account for correlations beyond first neighbors. The consideration of higher order dependence between neighboring bonds in coordinated motion necessitates the construction of multidimensional energy maps. A detailed analysis of a specific motion was carried out by Blomberg.[32] In his study, the simultaneous transition of three alter-

nating bonds in a sequence undergoing three-bond crankshaft motion was investigated. However, as the relative contribution of every possible transition to internal relaxation has to be considered, refinement in this direction would become increasingly complicated, particularly as the size of the motional unit increases.

The example calculations were carried out for the central bond of a nine-bond sequence in polyethylene. Clearly, the internal relaxation in polymers takes place by various modes involving sequences differing in size. A limited range of modes contributes to relaxation spectra in each experiment, depending on the specific characteristics of the experimental technique.[24,25] A rigorous analysis should consider not only motional units varying in size but also the location, within a motional unit, of the bond whose reorientation is detected, as is apparent from the comparison of results from optical and NMR experiments.[25]

Calculations performed but not included in the present study show that average relaxation time for internal units decreases with increasing sequence length. The same dependence on sequence length follows from the calculations carried out by Jernigan for α-ω-dibromo-n-alkanes with $n = 4$–6. The shorter relaxation time associated with longer sequences may be rationalized on the basis of the larger number of possible paths to relaxation which is available to longer sequences. Thus the decay in the internal orientational autocorrelation function is more rapid with longer sequences. The autocorrelation function calculated by Valeur et al.,[11] on the basis of three-bond motions, the shortest motions leaving the tails unchanged, was found to decay too slowly with time, which led them to append an additional exponential decay function to the derived equation. The present analysis demonstrates that a more rapid decay function is obtainable by allowing a longer sequence to undergo conformational transitions.

However another effect, the environmental resistance due to friction, tends to slow down the motion of the unit under consideration and this effect becomes increasingly stronger as the size of the motional unit increases. In fact, for Rouse-like modes the relaxation time is proportional to the second power of the molecular weight of the motional unit. Thus the application of the present analysis to sequences where Rouse-like behavior dominates is not meaningful. An upper bound for the size of the motional sequence is formulated in the form of a long-wavelength cutoff in the work of Bendler and Yaris.[25] The short-wavelength cutoff which is also introduced in their work is inherent in the present study since real molecular structures are considered.

Constraints operating on the ends of the sequence were found to exert a dramatic effect on $M_{2,int}(t)$. The slowing down of local dynamics upon precluding the large fluctuations of the sequence end-to-end vector was more accentuated at lower temperatures. Calculations also show that internal conformational rearrangements do not lead to complete relaxation as long as no external global reorientation is superposed on them. In fact, $M_{2,int}(t)$ converges to finite values that increase with the degree of constraints imposed by chain connectivity.

References and Notes

(1) Rouse, P. E., Jr. *J. Chem. Phys.* **1953**, *21*, 1272.
(2) Zimm, B. H. *J. Chem. Phys.* **1956**, *24*, 269.
(3) Verdier, P. H.; Stockmayer, W. H. *J. Chem. Phys.* **1962**, *36*, 227.

(4) Verdier, P. H. *J. Chem. Phys.* **1966**, *45*, 2118.

(5) Monnerie, L.; Gény, F. *J. Chim. Phys.* **1969**, *66*, 1961. Gény, F.; Monnerie, L. *Ibid.* **1969**, *66*, 1708. Gény, F.; Monnerie, L. *J. Polym. Sci., Polym. Phys. Ed.* **1979**, *17*, 131, 147.

(6) Helfand, E. *J. Chem. Phys.* **1978**, *69*, 1010. Helfand, E.; Wasserman, Z.; Weber, T. A. *Macromolecules* **1980**, *13*, 526.

(7) Hall, C. K.; Helfand, E. *J. Chem. Phys.* **1982**, *77*, 3275.

(8) Helfand, E. *J. Chem. Phys.* **1971**, *54*, 4651.

(9) Skolnick, J., Helfand, E. *J. Chem. Phys.* **1980**, *72*, 5489. Helfand, E.; Skolnick, J. *J. Chem. Phys.* **1982**, *77*, 5714.

(10) Orwoll, R. A.; Stockmayer, W. H. *Adv. Chem. Phys.* **1969**, *15*, 305.

(11) Valeur, B.; Jarry, J. P.; Gény, F.; Monnerie, L. *J. Polym. Sci., Polym. Phys. Ed.* **1975**, *13*, 667, 675, 2251.

(12) Jones, A. A.; Stockmayer, W. H. *J. Polym. Sci., Polym. Phys. Ed.* **1977**, *15*, 847.

(13) Boyer, R. F. *Rubber Chem. Technol.* **1963**, *34*, 1303. Schatzki, T. F. *J. Polym. Sci.* **1962**, *57*, 496; *Polym. Prepr. (Am. Chem. Soc., Div. Polym. Chem.)* **1965**, *6*(2), 646.

(14) Baysal, B.; Lowry, B. A.; Yu, H.; Stockmayer, W. H. In *Dielectric Properties of Polymers*; Karasz, F. E., Ed.; Plenum: New York, 1972; p 329.

(15) Stockmayer, W. H. *Pure Appl. Chem.* **1966**, *15*, 539.

(16) Matsuo, K.; Kuhlmann, K. F.; Yang, W. H.; Gény, F.; Stockmayer, W. H.; Jones, A. A. *J. Polym. Sci, Polym. Phys. Ed.* **1977**, *15*, 1347.

(17) Kramers, H. A. *Physica* **1940**, *7*, 284.

(18) Glauber, R. S. *J. Math. Phys.* **1963**, *4*, 294.

(19) Anderson, J. E. *J. Chem. Phys.* **1970**, *52*, 2821.

(20) Bozdemir, S. *Phys. Status Solidi B* **1981**, *103*, 459; *104*, 37.

(21) Skinner, J. L. *J. Chem. Phys.* **1983**, *79*, 1955; **1985**, *82*, 5232.

(22) Jernigan, R. L. In *Dielectric Properties of Polymers*; Karasz,

F. E., Ed.; Plenum: New York, 1972; p 99.

(23) Flory, P. J. *Statistical Mechanics of Chain Molecules*; Interscience: New York, 1969.

(24) Monnerie, L.; Lauprêtre, F. *Structure and Dynamics of Molecular Systems* Daudel, R., Ed.; D. Reidel: Dordrecht, 1986.

(25) Bendler, J. T.; Yaris, R. *Macromolecules* **1978**, *11*, 650. Skolnick, J.; Yaris, R. *Macromolecules*, **1982**, *15*, 1041; *15*, 1046.

(26) Hyde, P. D.; Waldow, D. A.; Ediger, M. D.; Kitano, T.; Ito, K. *Macromolecules* **1986**, *19*, 2533.

(27) This matrix $\mathcal{P}^{(N)}$ is the transpose of the conventional time-dependent transition probability matrix of Markov chains, where the *ij*th element is related to the conditional passage from state *i* at epoch t to state *j* at epoch τ with $\tau > t$. See, for example: Feller, W. *An Introduction to Probability Theory and its Applications*, 3rd ed.; Wiley: New York 1971; Vol I.

(28) Abe, A.; Jernigan, R. L.; Flory, P. J. *J. Am. Chem. Soc.* **1966**, *88*, 631.

(29) See, For example: Eyring, H. *J. Chem. Phys.* **1935**, *3*, 107. Wynne-Jones, W. F. K.; Eyring, H. *Ibid.* **1935**, *3*, 492; Glasstone, S.; Laidler, K. J.; Eyring, H. *The Theory of Rate Processes*; McGraw-Hill: New York, 1941; Chapter 4.

(30) The front factor has dimensions of $(length)^2/time$ according to the treatment of ref 9. Transformation to dimensions of $1/(time)$, required in the present treatment, was made upon dividing by $l^2 \sin^2 \theta$, where *l* is the bond length and θ is the supplemental bond angle. The numerical value of γ was taken as the mean of the corresponding values of trans and gauche conformations.

(31) Viovy, J. L.; Frank, C. W.; Monnerie, L. *Macromolecules* **1985**, *18*, 2606.

(32) Blomberg, C. *Chem. Phys.* **1979**, *37*, 219.

Structure of Many-Arm Star Polymers: A Molecular Dynamics Simulation

Gary S. Grest,[*†‡] **Kurt Kremer,**[†§] **and T. A. Witten**[†]

Corporate Research Science Laboratories, Exxon Research and Engineering Company, Annandale, New Jersey 08801, Institut für Physik, Universität Mainz, D-6500 Mainz, Federal Republic of Germany, and Institut für Festkörperforschung der Kernforschungsanlage Jülich, D-5170 Jülich, Federal Republic of Germany. Received October 20, 1986

ABSTRACT: We present a detailed simulation study of star polymers with many $(6 \le f \le 50)$ arms *f*. Each arm consists of $N = 50, 100,$ or 200 monomers. In most respects these show good agreement with the asymptotic scaling predictions of the Daoud–Cotton blob model. We report values for the universal ratios characterizing the scattering from such stars. We especially concentrate on many-arm properties and on deviations from recent scaling arguments and describe in detail anomalies in the structure factor. Because typical experimental systems have arm lengths that are on the border line to the asymptotic behavior, we expect that our results are relevant for the interpretation of experiments for both star polymers and micellar solutions.

I. Introduction

Branched polymers are important in our understanding of gels and rubber. Star polymers, one special class of branched polymers, have only recently been more intensively studied[1] following the progress of synthesizing such systems which has been made during the last few years. Star polymers are macromolecules where linear homopolymers are chemically attached to a seed or center molecule. The size of the seed is typically of the order of a bond length or somewhat larger but very small compared to the extension of the chains. Experimental stars were recently produced with up to 18 arms[2] connected to a single center. While using linear polymers with associating end groups, one can even produce starlike structures with many

more arms.[3] Theoretically the main interest up to now was concentrated on the asymptotic properties of stars in the limit of very long arms of *N* bonds per arm where the number of arms *f* is fixed. Although a scaling theory[4,5] and several field theoretical approaches[6–8] exist for such systems, little is known theoretically about the scattering of such objects. The only numerical studies[5,9,11,12] of these systems have concentrated on the critical exponents and the ratio of the mean-square radius of the star polymer to that of the linear polymer.[12] They have not investigated the static and dynamic structure function. Even less is known for systems with relatively few bonds *N* but many arms *f*. For such systems scaling arguments become somewhat ambiguous, and no analytic treatment is available up to now. This regime is important in light of the recent progress in synthesizing new stars and is already relevant for the investigation of dilute micellar structures.[3] For this reason, we have carried out a numerical and scaling study of star polymers in the regime where the

† Exxon Research and Engineering Co.

‡ Universität Mainz.

§ Institut für Festkörperforschung der Kernforschungsanlage Jülich.